DSCC2012-MOVIC2012-8720

MAXIMALLY-INFORMATIVE REGIONAL OCEAN MODELING SYSTEM (ROMS) NAVIGATION OF AN AUV IN UNCERTAIN OCEAN CURRENTS

Ross P. Anderson
Department of Applied Math & Statistics
University of California, Santa Cruz
Santa Cruz, California 95064
Email: anderson@soe.ucsc.edu

Georgi S. Dinolov
Department of Applied Math & Statistics
University of California, Santa Cruz
Santa Cruz, California 95064
Email: gdinolov@soe.ucsc.edu

Dejan Milutinović
Department of Applied Math & Statistics
University of California, Santa Cruz
Santa Cruz, California 95064
Email: dejan@soe.ucsc.edu

Andrew M. Moore
Department of Ocean Sciences
University of California, Santa Cruz
Santa Cruz, California 95064
Email: ammoore@ucsc.edu

ABSTRACT

The Regional Ocean Model System (ROMS) is a high dimensional computational model of ocean circulation. The model and data assimilation from various sources can provide a good estimate of ocean circulation variables, but not at a rate that is sufficient to track fast changes. For more frequent updates, we consider the use of an autonomous underwater vehicle (AUV) navigated along a maximally-informative path, i.e., one that maximally reduces uncertainty in ocean circulation variable estimations. The proposed solution deconstructs the problem into a long time-scale deterministic optimization problem for generating waypoints and a short time-scale stochastic optimal control problem for sequentially hitting these waypoints while taking into account the uncertainty of ocean currents. The latter is solved as a feedback control problem that is based on the stochastic Hamilton-Jacobi-Bellman equation and a locally consistent Markov chain approximation. Our results are illustrated by an example using data from the ROMS data assimilation.

NOMENCLATURE

$R(p_i)$	Reduction in ocean circulation uncertainty caused by visiting one point $p_i \in \mathbb{R}^2$
P^*	Maximally-informative path
P_N^*	Maximally informative path using N waypoints p_i
r	AUV-waypoint distance
φ	AUV-waypoint viewing angle
σ	Ocean current noise intensity
V_R	Constrained maximum distance between waypoints
D_R	Waypoint separation for uncertainty reduction

1 INTRODUCTION

The development of sophisticated autonomous underwater vehicles (AUVs) has opened the door to a variety of scientific, commercial, and military tasks, including mapping and sampling of environmental phenomena and spatiotemporal features, archaeological investigations, servicing of industrial infrastructure, and surveys of areas not accessible to tethered vehicles [1, 2]. In some cases, the operation of these vehicles is currently limited by the time allowed for data collection or by energy consumed by the vehicle, for example. Increasing trends in power capacity and cost effectiveness, however, will likely mitigate these limitations in the future [1]. Therefore, we consider the problem of finding a navigation strategy for a single AUV that provides maximally-informative observations of ocean circulation, that is, the measurements best improve the estimates of ocean circulation variables. Meanwhile, the motion of the AUV employing this navigation strategy should be robust to the uncertain ocean currents.

The ocean circulation estimates we consider are based on the Regional Ocean Modeling System (ROMS) [3–5], which is a large-scale computational dynamical model of ocean circulation and data assimilation with various sources of measurements, including satellites, ship observations, profiling floats, and tagged marine mammals. The most comprehensive measurements are those of the ocean surface temperature and surface elevation from satellites, which are typically available once per day. Sub-surface observations are typically available less frequently in space and time.

However, recent development of the ROMS and data assimilation shows that the ROMS can be used to compute how much a measurement at a certain ocean point can reduce the error of an ocean circulation variable estimate [5]. Consequently, an AUV can not only provide measurements at a rate necessary for more frequent updates of ROMS variables, but it can be navigated along the path providing a maximal reduction in estimation errors. We call this path *maximally-informative*, and for an easier visualization of results, we focus of 2D paths.

The problem of finding maximally-informative paths under limited resources has previously been considered in a number of ways. One well-known solution is the recursive greedy algorithm [6]. This algorithm gives the solution to the problem of finding a maximally-rewarding path on a directed graph with a submodular reward function under a constraint. This algorithm has strong theoretical performance guarantees and has been used in problems similar to ours with multiple robots [7]; modifications of the recursive greedy algorithm have also been developed [8, 9] in similar settings. Another graph-theoretic solution is an exhaustive search with branch and bound [10]. Other approaches to this problems involve local linear regression of variance [11], mixed integer programs [12], Rao-Black filters [13], and partially observable Markov processes [14].

In our ROMS-based problem formulation, finding the maximally-informative path leads to an ill-posed, non-Markovian optimization problem. Instead of introducing additional constraints or expanding the system state, we propose to decouple the original problem into a long time-scale deterministic kinematic problem of finding the optimal path waypoints, followed by a short time-scale stochastic optimal control problem for AUV navigation to these waypoints in the presence of unknown ocean currents. The authors have considered a similar stochastic optimal control problem of maintaining distance from a target with unknown future trajectory in [15].

This paper is organized as followed. In Section 2, we provide the problem formulation. The stochastic optimal control approach is presented in Section 3. Section 4 provides results, and conclusions are given in Section 5.

2 PROBLEM FORMULATION

Let us define a vehicle path on $\mathbb{R}^2$ as a sequence of points visited by the vehicle $\mathcal{P} = \{p_1, p_2, \ldots\}$, $p_i \in \mathbb{R}^2$. When the point p_i is visited, the uncertainty about ocean circulation reduces by
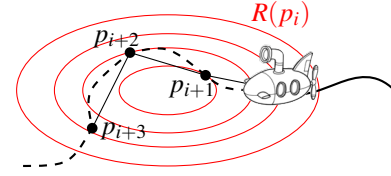

Figure 1. Illustration of an AUV following a maximally-informative path $\mathcal{P}_N^* = (p_1, p_2, \ldots, p_N)$ that reduces the uncertainty in ocean currents at point p_i by the quantity $R(p_i)$, which is shown by a set of contours. The distance between successive points is constrained to be less than V_R, while no information is gained from a point if it is within a distance D_R from a previously visited point.

an amount $R(p_i)$. These values are obtained from the ROMS data assimilation model and are assumed to be known. In the case when the path passes more than once through the same point, we assume that the error reduction at that point is the same as if the path had only passed through that point once. Our goal is to find the sequence of points defining a path that maximizes the total uncertainty reduction, and that can be executed by our vehicle. We call this path *the maximally-informative path $\mathcal{P}^*$*.

The total uncertainty reduction R_{tot} for a path $\mathcal{P}$ is given by

$$R_{tot}(\mathcal{P}) = R(p_1) + \sum_{i=2}^{} \left(R(p_i) \prod_{k=1}^{i-1} \phi(p_i, p_k) \right), \qquad p_i, p_k \in \mathcal{P} \tag{1}$$

where we use the window function ϕ based on the Euclidean vector norm $\|\cdot\|$ and radius D_R:

$$\phi(p_i, p_k) = \begin{cases} 0, & \|p_i - p_k\| \leq D_R \\ 1, & \text{otherwise,} \end{cases} \tag{2}$$

and where the path $\mathcal{P}$ satisfies the constraints given by underwater vehicle kinematics.

Since we consider paths in $\mathbb{R}^2$, the natural choice for the AUV kinematic model is

$$dx(t) = v\cos(\theta)dt + \sigma(x, y)dw_x \tag{3}$$

$$dy(t) = v\sin(\theta)dt + \sigma(x, y)dw_y \tag{4}$$

$$d\theta(t) = \frac{u}{\rho_{min}}dt, \qquad |u| \leq 1, \tag{5}$$

where dw_x and dw_y are increments of independent Wiener processes that take into account the uncertainty of ocean current-induced drift with location-dependent intensity $\sigma(x, y)$. The parameter ρ_{min} defines the intrinsic turning rate of the vehicle under a bounded control input in the absence of ocean currents.

The problem of finding the maximally-informative path $\mathcal{P}^*$ is to maximize the cost funtion (1) under kinematic constraints (3)-(5). As it stands, this is not a well-posed optimization problem since there are many solutions. Indeed, any path that passes

at least once through all possible points p_i will minimize R_{tot}. Moreover, this is a non-Markovian optimization problem since the cost function (1) depends on all points p_k visited prior to visiting p_i, $k < i$. However, the cost function (1) and (3)-(5) form the basis of an approach to compute the maximally-informative path $\mathcal{P}^*$ if we restrict the number of sample points p_i.

We thus propose to solve the problem based on a decomposition into a *deterministic*, long time-scale kinematic problem for computing a finite set of vehicle waypoints, and a *stochastic* feedback control problem for following the waypoints in the presence of uncertain ocean currents.

We define the *deterministic problem* as the problem of finding the sequence of N points $\mathcal{P}_N^* = \{p_1, p_2, ...p_N\}$ such that the cost function (1) is maximized under the following constraints:

$$\|p_{i+1} - p_i\| < V_R, \quad i \in 1, 2, ...N - 1 \tag{6}$$

$$p_1 = p_{\text{start}} \tag{7}$$

$$p_N = p_{\text{end}}, \tag{8}$$

where V_R is a maximum allowed distance between points, and p_{start} and p_{end} are given initial and final points, e.g., a dock or boat. Since the time between visiting the points is not constrained, the distance V_R is not directly connected to the vehicle velocity under the stochastic kinematics (3)-(5) and can be considered as an optimization parameter. This nonlinear optimization problem is prone to local minima, and so we solve this problem using a Simulated Annealing algorithm [16] (see Appendix A).

Once the points $p_1, \ldots, p_N$ are computed, the *stochastic optimal control problem* is to find a feedback control u for the kinematics model (3)-(5) so that starting from any point p_i (i.e., the current waypoint), the point p_{i+1}, corresponding to the next waypoint, is reached in minimum (expected) time.

While the deterministic part of the problem formulation can be solved as a nonlinear optimization problem, the stochastic optimal control solution is considered in the following section.

3 STOCHASTIC OPTIMAL CONTROL

The problem of reaching the point p_{i+1} from any initial condition can be defined as a problem of finding the control u in the kinematics model (3)-(5) that minimizes the expected time of arrival T at a target set (a ball) of radius δ around p_{i+1}. In this problem, it is necessary to give the target a nonzero radius since the probability of reaching a single point p_{i+1} under the kinematics model (3)-(5) is zero. The corresponding cost functional for this problem is

$$W(r, \varphi, u) = E\left\{ \int_0^T (1 + \varepsilon u^2) dt \right\}, \tag{9}$$

where r is the distance from the AUV to the point $p_{i+1} = \left[p_{i+1}^{(x)}, p_{i+1}^{(y)} \right]^T$ based on the Cartesian components $\Delta x = p_{i+1}^{(x)} - x$
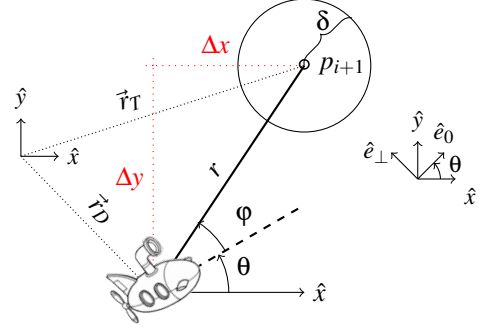

Figure 2. Diagram of an AUV at position $\vec{r}_D$ that is moving at heading angle θ in order to converge on a target at $\vec{r}_T$ in minimum time in the presence of currents. The target set is shown as a circle of radius δ about the target.

and $\Delta y = p_{i+1}^{(y)} - y$, and φ is the angle between the AUV heading angle and the direction to point p_{i+1} (see Fig. 2):

$$r = \sqrt{(\Delta x)^2 + (\Delta y)^2} \tag{10}$$

$$\varphi + \theta = \arctan\left(\frac{\Delta y}{\Delta x}\right). \tag{11}$$

We apply a small quadratic penalty ε to the control. The control will drive the AUV to the target set, and upon reaching this set, all motion, control, and cost cease. At this point, the target set center is fixed at the next point p_{i+2}, and we apply the same control used to converge on the point p_{i+1}, using the new relative coordinates r and φ.

Next, consider the differentials of the Cartesian components Δx and Δy of the distance r:

$$d(\Delta x) = -dx = -v\cos(\theta)dt - \sigma(x,y)dw_x \tag{12}$$

$$d(\Delta y) = -dy = -v\sin(\theta)dt - \sigma(x,y)dw_y. \tag{13}$$

Assuming that the noise intensities are a known constant $\sigma(x,y) = \sigma$ and applying Itō's lemma to (3)-(5) and (12)-(13), we can find the differentials dr and $d\varphi$ as (see Appendix B):

$$dr(t) = \left(-v\cos(\varphi) + \frac{\sigma^2}{2r} \right) dt + \sigma dw_0 \tag{14}$$

$$d\varphi(t) = \left(\frac{v}{r}\sin(\varphi) - \frac{u}{\rho_{\min}} \right) dt + \frac{\sigma}{r} dw_\perp, \tag{15}$$

where dw_0 and $dw_\perp$ are increments of mutually independent Wiener processes along the vector connecting the AUV and the waypoint and normal to it, respectively (see Fig. 2).

For a shorter notation, let us define the state vector as $\mathbf{x} =$

$[r,\varphi]^T$ and the differential operator $\mathcal{L}^u$ as

$$\mathcal{L}^u = \sum_{i=1}^{2} b_i(\mathbf{x})\frac{\partial}{\partial x_i} + \frac{1}{2}\sum_{i,j=1}^{2} a_{ij}(\mathbf{x})\frac{\partial^2}{\partial x_i \partial x_j}, \qquad (16)$$

written in terms of mean drift $\mathbf{b}(\mathbf{x}) \in \mathbb{R}^2$ and diffusion matrix $\mathbf{a}(\mathbf{x}) \in \mathbb{R}^{2x2}$:

$$\mathbf{b}(\mathbf{x}) = \begin{bmatrix} -v\cos(\varphi) + \frac{\sigma^2}{2r} \\ \frac{v}{r}\sin(\varphi) - \frac{u}{\rho_{\min}} \end{bmatrix}, \qquad \mathbf{a}(\mathbf{x}) = \begin{bmatrix} \sigma^2 & 0 \\ 0 & \sigma^2/r^2 \end{bmatrix}, \quad (17)$$

where $a_{ij} = 0$ for $i \neq j$ since increments dw_0 and $dw_\perp$ are mutually independent. It can be shown that a sufficiently smooth $W(\mathbf{x}, u)$ given by (9) satisfies

$$\mathcal{L}^u W(\mathbf{x}, u) + 1 + \varepsilon u^2 = 0, \qquad (18)$$

and that the stochastic Hamilton-Jacobi-Bellman (HJB) equation for the minimum cost-to-go $V(\mathbf{x})$ over all controls is

$$\inf_{u \leq 1}\left[\mathcal{L}^u V(\mathbf{x}) + 1 + \varepsilon u^2\right] = 0. \qquad (19)$$

We solve (19) using a discrete-time and discrete-state Markov chain approximation [17] whose transitions are locally consistent with the original controlled process (14)-(15) with respect to the cost $W(\mathbf{x}, u)$ mean value and variance evolutions. The iterative formula for value iteration on the optimal cost-to-go function for states $\mathbf{x} \in \mathbb{X} \setminus \partial\mathbb{X}$ in the computational domain $\mathbb{X}$ inside boundaries $\partial\mathbb{X}$ is then

$$V^h(\mathbf{x}) = \min_{u \leq 1}\left\{\sum_{i=1}^{2} p(\mathbf{x} \pm e_i h | \mathbf{x}, u)V^h(\mathbf{x} \pm e_i h)\right.$$
$$\left. + \left(1 + \varepsilon u^2\right)\Delta t^h(\mathbf{x}, u)\right\}, \qquad (20)$$

where e_i is the standard basis vector (for r or φ) and h is the step size in the respective direction. Here, the Markov chain transition probabilities $p(\cdot|\cdot)$ are given by

$$p(r \pm h, \varphi | r, \varphi, u) = \Delta t^h(\mathbf{x}, u)\left[\frac{\sigma^2}{2h^2} + \frac{\left(-v\cos\varphi + \frac{\sigma^2}{2r}\right)^{\pm}}{h}\right]$$

$$p(r, \varphi \pm h | r, \varphi, u) = \Delta t^h(\mathbf{x}, u)\left[\frac{\sigma^2}{2(rh)^2} + \frac{\left(\frac{v}{r}\sin\varphi - \frac{u}{\rho_{\min}}\right)^{\pm}}{h}\right]$$
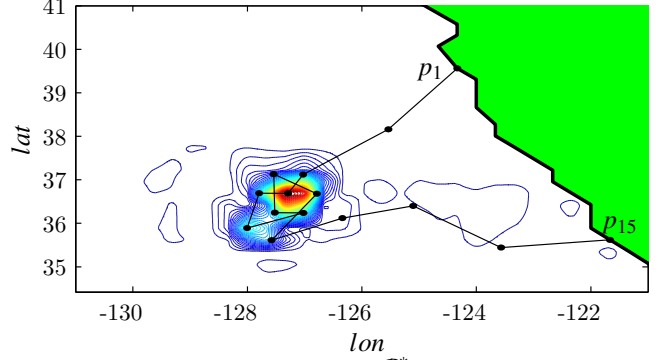
$$f^{\pm} = \max\{0, \pm f\}, \qquad (21)$$

Figure 3. Maximally-informative path $\mathcal{P}_N^*$ on the uncertainty reduction field $R(p_i)$ as computed by simulated annealing, $N = 15$. The green is a land mass on which the first and last points p_1 and p_{15} must lie.

and the interpolation time interval is

$$\Delta t^h(\mathbf{x}, u) = \left[\frac{\sigma^2}{h^2} + \frac{\sigma^2}{(rh)^2} + \frac{\left|-v\cos\varphi + \frac{\sigma^2}{2r}\right|}{h} + \frac{\left|\frac{v}{r}\sin\varphi - \frac{u}{\rho_{\min}}\right|}{h}\right]^{-1}. \qquad (22)$$

The computational domain $\mathbb{X}$ in this problem is semi-periodic; the points on the boundary $\varphi = \pi$ and $\varphi = -\pi$ are identical, i.e., $(r, \pi) = (r, -\pi)$ for any r. For those states $\mathbf{x} \in \partial\mathbb{X}$ along the boundary of the domain, we apply absorbing boundary conditions:

$$V(r, \varphi) = \begin{cases} 0 & \text{if } r \leq \delta \\ 100 & \text{if } r = r_{\max} > V_R, \end{cases}$$

where the absorbing state at $r = r_{\max}$ is penalized in order to keep the AUV within $\mathbb{X}$.

4 RESULTS

In this section, we present the results our approach applied to the estimation of an ocean circulation variable – the 7-day average ocean water transport crossing the 37N parallel in the 500m-thick layer below the ocean surface. The squared error reduction function $R(p_i)$ was obtained from a linear interpolation over the data provided through the ROMS data assimilation model. Since these data were primarily flat except in a concentrated region (Fig. 3), a small Gaussian of covariance 50, centered on the peak of the ROMS data, was added in order to facilitate optimization. Next, a simulated annealing algorithm [16] was applied to the cost function (1) and constraints (6)-(8) in order to produce 15 points $p_1, \ldots, p_{15}$ that together define the maximally-informative path $\mathcal{P}_N^*$. Details for this algorithm may be found in Appendix A. The minimum distance between points was chosen as $D_R = 0.3$ and the maximum as $V_R = 2$. Figure 3 shows the computed set of points given the fixed starting and end locations p_1 and p_{15}
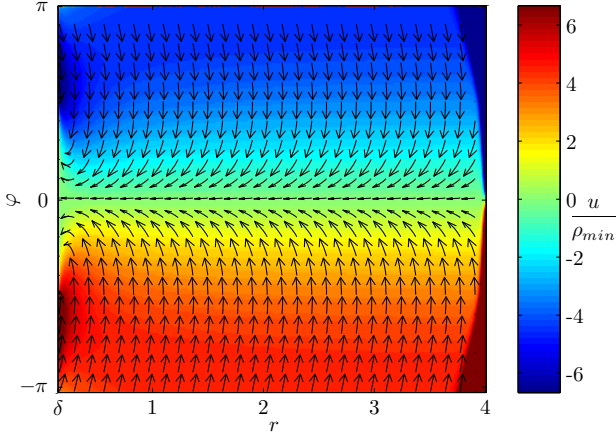
4

Figure 4. Stochastic optimal feedback control $u = u(r, \varphi)$ based on current distance and viewing angle to the target p_{i+1}.
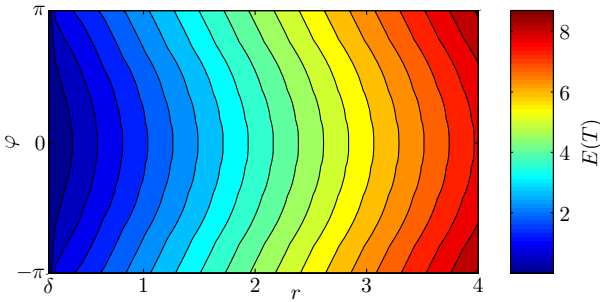

Figure 5. Expected value of the time required to hit one target based on its initial condition in the stochastically-varying currents. Level sets were computed from the backward Kolmogorov equation [18].

along a coastline. It is seen that in the area with maximum uncertainty reduction, the waypoints are minimally spaced. Note that because of the cost function, any path through these points would result in the same reduction in the squared error of ocean variables, but that the indicated path is feasible for the AUV kinematics.

Next, the stochastic optimal feedback control for the vehicle was computed using the methods of the previous section, with $v = 0.15, \sigma = 0.05, \varepsilon = 0.1$, and $\rho_{min} = 0.15$. Value iterations were stopped after the change in the cost-to-go function $V(r, \varphi)$ was less than 10^{-10}. Figure 4 shows the resulting optimal control as a function of the distance and viewing angle to the next waypoint p_{i+1}. It can be seen that after reaching a target set centered on p_i, the control will attempt to orient the AUV toward the next waypoint p_{i+1}, i.e., φ is pushed to 0, at which time the AUV will head toward the waypoint. However, due to the unknown ocean currents that are assumed to be random, the AUV may be aided or impeded in this task. Along these lines, Fig. 5 shows the expected value of the time of arrival at a waypoint p_{i+1} based on the relative position in which the AUV finds itself after reaching

p_i. It should be noted that a similar control law to that in Fig. 4 is also seen for larger values of σ. Additionally, if the radius of the target set is chosen to be smaller than the minimum AUV turning radius, the optimal control will contain regions in (r, φ) that instruct the AUV to first distance itself from the target before attempting another approach. However, we did not feel that this was a realistic scenario for the application under consideration.

Once the waypoints comprising the maximally-informative path $\mathcal{P}_N^*$ have been obtained and the stochastic feedback control has been computed, the AUV trajectory is that path which arises when consecutively applying the optimal control to reach the sequence of points in $\mathcal{P}_N^*$. Figure 6(a) shows the resulting AUV path when hitting these waypoints in the absence of ocean currents.

To test these methods against an ocean current, a scalar field $\Phi(\mathbf{x})$ on a discrete state space $\mathbf{x} \in (\mathbf{x}_1, \mathbf{x}_2, \ldots, \mathbf{x}_n)$ was randomly sampled from a Gaussian Process (GP), which describes a distribution over smooth functions $\Phi(\mathbf{x})$, using an exponential covariance function

$$Cov(\Phi(\mathbf{x}_i), \Phi(\mathbf{x}_j)) = \sigma \sqrt{\frac{2}{\pi}} \exp\left\{ -50(\mathbf{x}_i - \mathbf{x}_j)^T (\mathbf{x}_i - \mathbf{x}_j) \right\}.$$

Then the ocean current used in simulation was computed from the gradient of $\Phi(\mathbf{x})$ (cf. (3)-(4)):

$$dx(t) = v\cos(\theta)dt + \nabla_x \Phi(x, y)dt$$
$$dy(t) = v\sin(\theta)dt + \nabla_y \Phi(x, y)dt.$$

In simulation, the current was interpolated from its values in the discrete state space of the GP, and the resulting AUV path may be seen in Fig. 6(b). Note that although the AUV path changed from that in Fig. 6(a) due to the ocean currents, the stochastic control, which "anticipates" the unknown variation in ocean current, was sufficient to keep the AUV on track, without requiring multiple attempts to hit any waypoint. The resulting trajectory for hitting the same targets in a more variable ocean current ($\sigma = 0.25$) is also seen in Figure 6(c), using control computed for $\sigma = 0.25$.

5 CONCLUSIONS

This work considers the problem of computing the AUV path that leads to maximum uncertainty reduction in the estimates of ocean circulation variables, as described by the ROMS data assimilation model. This defines an ill-posed, non-Markovian optimization problem for the maximally-informative path. To this end, we deconstructed the problem into two subproblems, the first of which computes an optimal sequence of waypoints that the AUV is capable of hitting, and a secondary stochastic feedback control problem, whereby the AUV is then controlled to consecutively hit each the target around each waypoint in the presence of uncertain ocean currents. The control
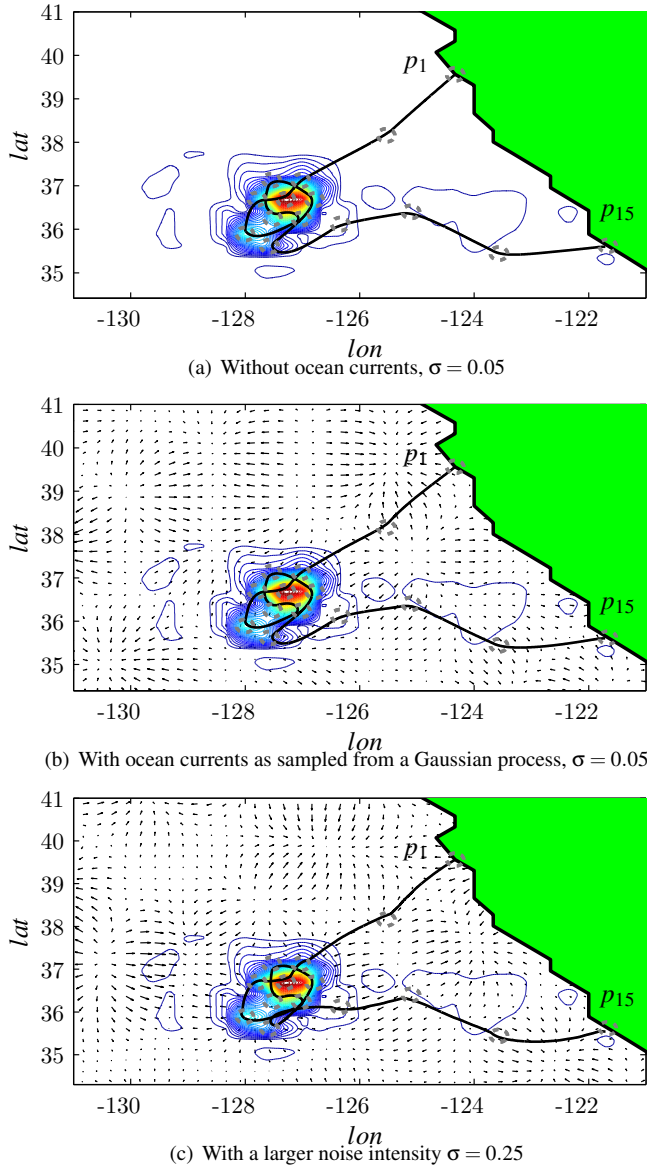
5

Figure 6. Simulation of an AUV visiting locations $p_1 \ldots, p_{15}$ of the maximally-informative path $\mathcal{P}_N^*$. Target points are shown as dashed circles, and the AUV path is in black. The ROMS uncertainty reduction $R(p_i)$ are shown as contours, and the green is a land mass on which the first and last points p_1 and p_{15} must lie.

was computed from a Markov chain approximation to the HJB equation, and simulations indicate that the motion of the AUV is robust to unknown ocean currents. Future work will consider the uncertainty reduction along the continuous AUV path and navigation of multiple AUVs.

ACKNOWLEDGMENT

REFERENCES

[1] Antonelli, G., Fossen, T., and Yoerger, D., 2008. "Underwater Robotics". In *Springer Handbook of Robotics*, B. Sciliano and O. Khatib, eds. ch. 43, pp. 987–1008.

[2] Wood, S., 2009. "Autonomous underwater vehicles". In *Intelligent Underwater Vehicles*, A. Inzartsev, ed. I-Tech Education and Publishing KG, ch. 26.

[3] Moore, A., Arango, H., Miller, A., Cornuelle, B., DiLorenzo, E., and Neilson, D., 2004. "A comprehensive ocean prediction and analysis system based on the tangent linear and adjoint components of a regional ocean model". *Ocean Modelling, 7*, pp. 227–258.

[4] Shchepetkin, A., and McWilliams, J., 2005. "The regional ocean modeling system: A split-explicit, free-surface, topography following coordinates ocean model". *Ocean Modelling, 9*, pp. 347–404.

[5] Moore, A., Arango, H., and Broquet, G., 2011. "Analysis and forecast error estimates derived from the adjoint of 4d-var (revised and under review)". *Monthly Weather Review*.

[6] Chekuri, C., and Pal, M., 2005. "A recursive greedy algorithm for walks in directed graphs". In Proceedings of the 46th Annual IEEE Symposium on Foundations of Computer Science (FOCS), IEEE, pp. 245–253.

[7] Meliou, A., Krause, A., Guestrin, C., and Hellerstein, J., 2007. "Nonmyopic informative path planning in spatio-temporal models". In Proceedings of the 22nd AAAI Conference on Artificial Intelligence, AAAI, pp. 602–607.

[8] Singh, A., Krause, A., Guestrin, C., Kaiser, W., and Batalin, M., 2007. "Efficient planning of informative paths for multiple robots". In Proceedings of the 20th International Joint Conference on Artificial Intelligence, pp. 2204–2211.

[9] Singh, A., Krause, A., and Kaiser, W. "Nonmyopic adaptive informative path planning for multiple robots". In Proceedings of the 21st International Joint Conference on Artificial Intelligence, pp. 1843–1850.

[10] Jonathan, B., and Sukhatme, G., 2011. "Branch and bound for informative path planning". In Proceedings of the 2011 IEEE International Conference on Robotics and Automation, IEEE.

[11] Zhang, B., and Sukhatme, G., 2007. "Adaptive sampling for estimating a scalar field using a robotic boat and a sensor network". In Proceedings of the 2007 IEEE International Conference on Robotics and Automation, IEEE, pp. 3673–3680.

[12] Yilmaz, N., Evangelinos, C., Lermusiaux, P., and Patrikalakis, N., 2008. "Path planning of autonomous underwater vehicles for adaptive sampling using mixed integer linear programming". *IEEE Journal of Oceanic Engineering, 33*(4), pp. 522–537.

[13] Stachniss, C., Grisetti, G., and Burgard, W., 2005. "Information gain-based exploration using rao-blackwellized particle filters". In Proceedings of Robotics: Science and Systems (RSS), pp. 65–72.

[14] Roy, N., Gordon, G., and Thrun, S., 2005. "Finding ap-

Algorithm 1 Determine optimal sequence of waypoints $\mathcal{P}_N^*$

$\mathcal{P}_N \leftarrow \{p_{\text{start}}, \ldots, p_{\text{end}}\}$ ▷ initial guess
$\tau \leftarrow 100$ ▷ initial temperature
$E \leftarrow R_{tot}(\mathcal{P}_N)$ ▷ initial cost
while $\tau \geq 1 \times 10^{-8}$ **do**
     $n_{\text{attempts}} \leftarrow n_{\text{attempts}} + 1$
     if $n_{\text{attempts}} \geq 2000$ or $n_{\text{success}} \geq 20$ **then**
         $\tau \leftarrow 0.99\tau$
         $n_{\text{attempts}} \leftarrow 1$
         $n_{\text{success}} \leftarrow 1$
     end if
     repeat
         sample $i \sim \{2, \ldots, N-1\}$
         $\mathcal{P}_N' \leftarrow \{p_1, \ldots, p_{i-1}, N(p_i, .0001), p_{i+1}, \ldots, p_N\}$.
         $E' \leftarrow R_{tot}(\mathcal{P}_N')$
     until constraints (6)-(8) satisfied
     if $\exp((E - E')/\tau) > \text{Uni}[0,1]$ **then**
         $E \leftarrow E'$
         $\mathcal{P}_N \leftarrow \mathcal{P}_N'$
         $n_{\text{success}} \leftarrow n_{\text{success}} + 1$
     end if
end while
$\mathcal{P}_N^* \leftarrow \mathcal{P}_N$ ▷ Optimal sequence of waypoints

---

proximate pomdp solutions through belief compression". *Journal of Artificial Intelligence Research,* **23**, pp. 1–40.

[15] Anderson, R., and Milutinović, D., 2011. "Dubins vehicle target tracking of a target with unpredictable trajectory". In Proceedings of the 4th ASME Dynamic Systems and Control Conference, IEEE.

[16] Kirkpatrick, S., 1983. "Optimization by simulated annealing". *Science,* **220**.

[17] Kushner, H., and Dupuis, P., 2001. *Numerical methods for stochastic control problems in continuous time*. Springer.

[18] Gardiner, C., 2009. *Stochastic Methods: A Handbook for the Natural and Social Sciences*, 4th ed. Springer.

Appendix A: Description of Simulated Annealing Algorithm

Here we briefly describe the simulated annealing algorithm used to compute the optimal sequence of points $\mathcal{P}_N^* = \{p_1, \ldots, p_N\}$. The total uncertainty reduction function $R_{tot}(\mathcal{P}_N)$ likely has many local minima, and this algorithm attempts to avoid a greedy solution that descends the gradient of $R_{tot}(\cdot)$ by allowing for guesses of the path $\mathcal{P}_N$ which increase $R_{tot}(\cdot)$. The extent to which these guesses can increase $R_{tot}(\cdot)$ is gradually decreased according to a so-called cooling schedule. For this algorithm, the cooling schedule for temperature τ was chosen as

$\tau_{n+1} = 0.99\tau_n$, with $\tau_0 = 100$, and new path configurations were generated by randomly perturbing one point $p_i \in \mathcal{P}_N$ at a time with a normally-distributed random variable with standard deviation 0.01. Pseudocode may be found in Algorithm 1.

Appendix B: Derivation of (14)-(15)

Beginning with the evolution of the Cartesian components Δx and Δy, (12)-(13), the total differential for r (10) can be found using Itō's lemma as:

$$
\begin{aligned}
dr = & \frac{\Delta x}{r} d(\Delta x) + \frac{\Delta y}{r} d(\Delta y) \\
& + \frac{1}{2}\left(\frac{1}{r} - \frac{(\Delta x)^2}{r^3}\right)(d(\Delta x))^2 \\
& + \frac{1}{2}\left(\frac{1}{r} - \frac{(\Delta y)^2}{r^3}\right)(d(\Delta y))^2 \\
& - \frac{(\Delta x)(\Delta y)}{r^3}(d(\Delta x))(d(\Delta y)).
\end{aligned} \tag{23}
$$

With substitution of partial derivatives and by taking into account that $\cos(\theta + \varphi) = \Delta x/r$ and $\sin(\theta + \varphi) = \Delta y/r$ (see Fig. 2), it can be shown that

$$
\begin{aligned}
dr = & \left(-v_A \cos\varphi + \frac{\sigma^2}{2r}\right) dt \\
& + \sigma \cos(\theta + \varphi) dw_x + \sigma \sin(\theta + \varphi) dw_y.
\end{aligned} \tag{24}
$$

Similarly, from (11), the total differential of $\varphi + \theta$ is

$$
\begin{aligned}
d(\theta + \varphi) = & -\frac{\Delta y}{r^2} d(\Delta x) + \frac{\Delta x}{r^2} d(\Delta y) \\
& + \frac{(\Delta x)(\Delta y)}{r^4}(d(\Delta x))^2 - \frac{(\Delta x)(\Delta y)}{r^4}(d(\Delta y))^2 \\
= & \frac{v_A}{r} \sin\varphi \, dt \\
& - \frac{\sigma}{r} \sin(\theta + \varphi) dw_x + \frac{\sigma}{r} \cos(\theta + \varphi) dw_y.
\end{aligned} \tag{25}
$$

Since the components dw_x and dw_y of the original stochastic process model are symmetric, it follows that the noise is invariant to a coordinate frame rotation by $\varphi + \theta$ [18]. In (24) and (25), it is seen that the stochastic terms are multiplied by such a rotation matrix, and so we define new independent Wiener process increments dw_0 and $dw_\perp$, corresponding to motion in the direction of $\varphi + \theta$ and perpendicular to it. Replacing the stochastic terms in (24) and (25) with their corresponding transformed terms leads to the relative AUV-waypoint kinematics model (14)-(15).